2026 IEEE International Conference on Robotics and Automation (ICRA 2026)
June 1-5, 2026. Vienna, Austria

Ringbot Quad: A Monocycle Robot with Four Legs for versatile wheel-leg transformable locomotion

Kevin G. Gim and Joohyung Kim

Abstract— **Integrating multiple locomotion modes on a single platform has become an active focus in pursuit of versatile and efficient movement. This paper introduces a novel monocycle robot with four legs, named Ringbot Quad, combining the wheeled and legged mechanisms. The Ringbot Quad is developed as a unique monocycle mechanism that replaces the traditional monocycle drivetrain with four individually actuated driving modules, each topped with an articulated leg. The four legs can be used for balance and steering in driving mode and for quadruped walking that fully supports the body with the legs. By switching between two distinct locomotion modes, it can navigate various terrains and overcome obstacles typically challenging for either mechanism alone. In this work, we present a compact-scale Ringbot Quad prototype as a proof of concept for the proposed mechanism, demonstrating the feasibility of a new type of mobile robot.**

I. Introduction

The pursuit of advanced mobility in autonomous robotics has been a driving force in the field of robotics and mechatronics, leading to innovations that challenge conventional paradigms. This trend has increasingly focused on developing robots capable of versatile movement, by incorporating multiple locomotion modes within a single platform.

One of the most active approaches combines wheeled and legged mechanisms. Legged mechanisms, the predominant form of locomotion in animals, use limbs to support the body and maneuver by moving the supporting points. Reflecting nature's adaptive evolution, the legged mechanism offers versatile locomotion capabilities, enabling it to navigate various obstacles and terrains. However, despite its versatility, legged locomotion tends to be less energy-efficient, with the constant weight-bearing and discrete movements leading to vibrations and mass fluctuations, which can limit speed and payload capacity.

Wheeled mechanisms, a key human invention, offer greater energy efficiency and smoother, faster travel through continuous rolling, but they struggle with obstacles, vertical offsets, and gaps. To address these limitations, researchers began exploring combined legged and wheeled systems. The 2015 DARPA Robotics Challenge [1]–[3] showcased this integration, with robots like ETH Zurich's quadruped using wheels on their legs [4] for versatile movement. Additionally, some robots featured innovative designs, such as transformable and spherical quadrupeds, to switch between locomotion mode [5], [6].

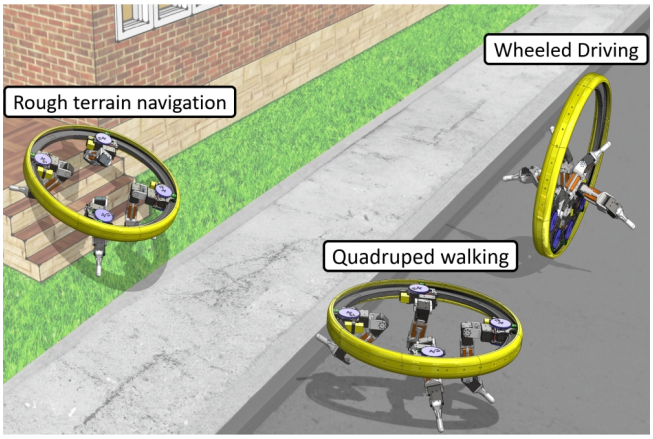

Fig. 1: Illustration of Ringbot Quad's navigation on various scenarios

In pursuit of a versatile mobile robot platform combining wheeled and legged mechanisms, we adopted the monocycle mechanism. By shifting the weight inside the wheel, driving torque can be generated. The large wheel offers superior obstacle navigation with a small footprint. Moreover, monocycle mechanism has inherent pitch stability, as its center of mass (CoM) is lower than its rotational axis, naturally seeking equilibrium. Unlike a unicycle, which has a higher CoM and requires significant control for balance, the monocycle's lower CoM provides intrinsic stability with lower energy demands [7].

Past developments in monocycle robots have incorporated gyroscopic flywheels for stabilization and steering [8]–[10] and ballast pendulums for balance [11], but despite their innovative design and control strategies, these systems often faced limitations such as energy inefficiency from maintaining flywheel momentum, restricted balancing correction capabilities, and inadequate internal space for practical applications.

Ringbot is a monocycle robot with a leg mechanism that was previously developed [12]. Ringbot features a large monocycle wheel and two independently actuated driving modules, each equipped with a leg on top. These modules move within the wheel, generating power for driving. The two legs facilitate steering by shifting the robot's weight during movement and also enable legged motions such as self-righting, fall prevention, and holonomic turns.

In this work, we introduce Ringbot Quad, a monocycle robot with four legs that combines both monocycle driving

Kevin Gim was with the KIMLAB (Kinetic Intelligent Machine Lab), University of Illinois Urbana-Champaign, IL 61801, USA. He is now with Boston Dynamics, Waltham, MA 02451, USA (email: kevingim89@gmail.com).
Joohyung Kim is with the KIMLAB, University of Illinois, Urbana-Champaign, IL 61801, USA (email: joohyung@illinois.edu).

and quadrupedal walking by fully supporting its body with its legs. Unlike the two-legged version, where the legs primarily assist in driving, the four-legged model allows for complete quadrupedal walking, offering two distinct locomotion modes. The versatile mobility of Ringbot Quad enables it to navigate varied terrains, particularly in urban settings with roads, sidewalks, and curbs, as shown in Fig. 1. Its compact size and agility make it ideal for maneuvering through crowded spaces, with potential applications in automated tasks like last-mile delivery.

In this paper, we present a compact-scale prototype as a proof of concept for the proposed mechanism and controller. The primary objective of this work is to demonstrate a novel and creative approach to mobile robot design, highlighting the feasibility and potential of combining distinct locomotion modes within a unified platform. The paper is structured to offer an in-depth understanding of the Ringbot Quad's development process, encompassing the details of hardware and implementation of driving and walking controllers, the design optimization process, and the conclusive results of the developed system.

II. Mechanism Design

A. Wheel

The wheel itself, with a diameter of 515 mm and a weight of 1.145 kg, is constructed by 3D printing multiple segments and assembling them into a spokeless wheel structure as shown in Fig. 2a. The inner ring segments, serving as the rail for the driving modules, demand high geometric precision and stiffness. Therefore, they were printed using micro carbon fiber-filled nylon material at a layer height of 50 microns. To enhance the wheel's structural integrity, layers of continuous carbon fiber reinforcement are integrated into the 3D-printed inner segments. This enhancement prevents distortion from leg movements, ensuring stable driving performance. Additionally, during quadrupedal walking, the wheel must withstand considerable load and impacts, necessitating robust strength and stiffness. To further reinforce the ring structure and prevent segment separation, carbon fiber tubes are placed inside the wheel assembly, running along their length.

The outer ring parts of the wheel function as the tire, making direct contact with the ground. This tire is designed with a wide profile to provide a substantial stability margin, allowing the Ringbot to stand upright and be less susceptible to lateral disturbances. The segments forming the outer ring are printed with PLA (Polylactic Acid), offering a cost-effective solution for the robot's fabrication. Similar to the inner ring, two carbon fiber tubes are integrated within the outer ring part to prevent separation and increase stiffness.

B. Driving Module

The driving module is a key component in the Ringbot system, replacing the driving components in the conventional monocycle mechanism. This module is securely mounted on the rail of the inner ring parts using multiple bearings, allowing it to move with only 1-DOF along the rail, around the wheel's inner circumference. Securing the driving module

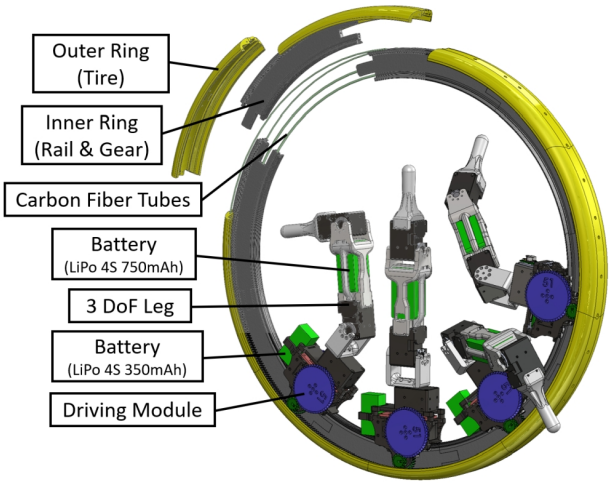

(a) Whole view

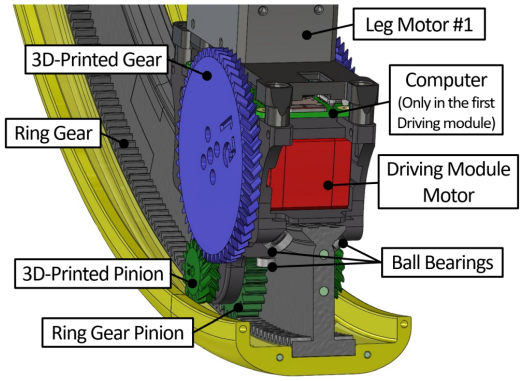

(b) Driving Module

Fig. 2: 3D CAD model of Ringbot Quad

with multiple bearings on the rail effectively reduces any slack between the module and the rail, while also ensuring low friction. This precise mating is essential for driving performance but also important for ensuring the accuracy of legged motion.

Each driving module contains two synchronized servo motors (DYNAMIXEL XC330-T077-T) that move it along the rail. A 3D-printed gearset, attached to the output of each motor, amplifies the motor's speed, enabling faster driving and sufficient angular momentum for gyroscopic stability. The low-profile, 3D-printed gears use a Herringbone structure for increased strength and efficiency. These gears engage with the ring gear on the wheel's inner surface.

The driving motor must provide sufficient speed to generate enough gyroscopic force to stabilize the robot in driving mode, while also delivering adequate torque to overcome stiction friction as the driving module begins its movement. Additionally, for legged motion, the motors need to maintain precise position control as they function as the primary joint in the leg chain. To meet these requirements, we installed two identical servo motors in each driving module and synchronized their movements via the motor controller firmware. Although dual-motor actuation was used to drive

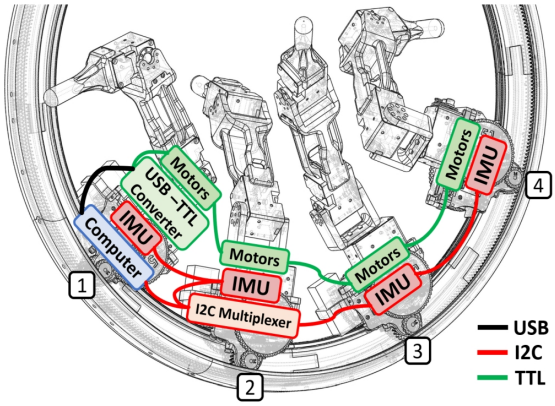

(a)

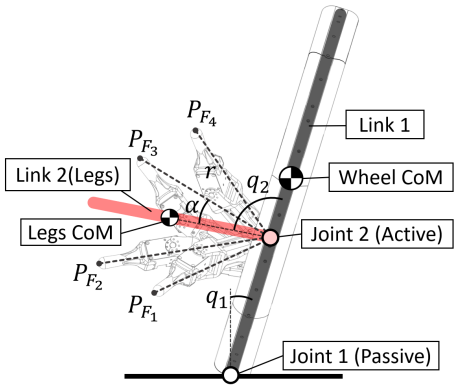

(b)

Fig. 3: (a) Diagram illustration of the integrated network of computing, sensors, and electronic components within the communication architecture (b) Simplified lateral dynamic model

the module, there exists a trade-off between torque and speed determined by the gear ratio of the drive train. Each motor provides a maximum power of only 10 W, resulting in a combined output of 20 W—barely sufficient to overcome the friction between the rim gear and module gear, while also needing to spin fast enough to generate the gyroscopic force required for stabilization. This power limitation stems from the compact scale of the current prototype, which can be resolved in a larger-scale implementation. By supplying a higher voltage (15V) than the motor's rated 12V, we achieved a maximum driving speed of 4 km/h at 290 RPM.

In Ringbot Quad, there are four driving modules, driving independently. Although their configurations are almost the same with each other, there are slight variations in the onboard electronics for each module. The electronic system network of the Ringbot Quad system is depicted in Fig. 3a. A single board computer (Raspberry Pi Zero 2 W) is mounted on the first driving module, operating the entire robot system. The computer communicates to all the servo motors in the system via TTL (Transistor-Transistor Logic) communication, allowing them to be interconnected in a daisy chain. The first driving module also includes a USB-TTL converter board that links the motors to the computer.

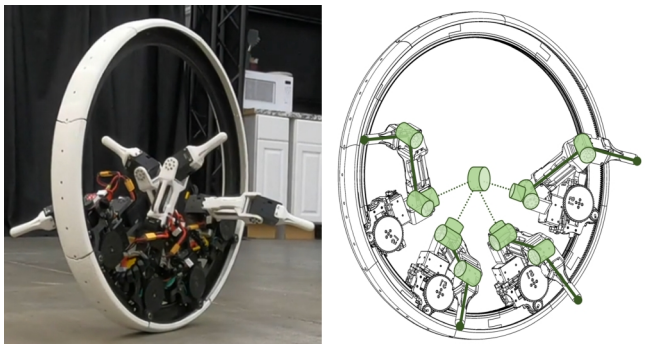

(a) Driving mode

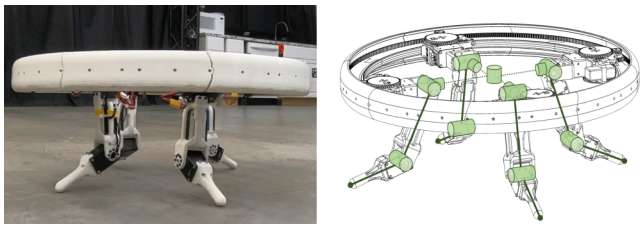

(b) Quadruped mode

Fig. 4: Leg joint configuration of Ringbot Quad

Each driving module in the Ringbot Quad is equipped with an individual Inertial Measurement Unit (BNO055) capable of measuring each module's absolute orientation, resulting in the system having four independent IMU measurements. An I2C multiplexer board, installed on the second driving module, connects to all four IMUs, permitting a single computer to effectively process signals from each unit through a single I2C channel. This arrangement simplifies the wiring between driving modules, reducing complexity and increasing the robustness of signal connections.

C. Leg

Each driving module in the Ringbot Quad is equipped with a 3-DOF leg mounted on top, actuated by three servo motors (DYNAMIXEL XM430-W210-T). These motors operate on the same serial channel as the driving motors, simplifying the integration of sensors and motor drivers and allowing for a more compact driving module system.

The leg topology of the Ringbot Quad is optimized for lateral shift movements as an inverted pendulum when the wheel is upright in driving mode. In quadrupedal mode, when the wheel lies parallel to the ground, the legs enable walking motion while fully lifting the body. Fig. 4 illustrates the leg's joint structure in both driving and quadruped modes. The movement of the driving module acts as a first leg joint with a linkage that connects the wheel centroid and each driving module.

In driving mode, each driving module's speed is controlled to drive the wheel, and simultaneously, the positions of the first virtual leg joints are also manipulated to keep a consistent distance between them. On the other hand, in quadruped walking mode, the driving modules take on symmetric positions, maintaining equal distances at 90-degree intervals. Therefore in both modes, the joint angles

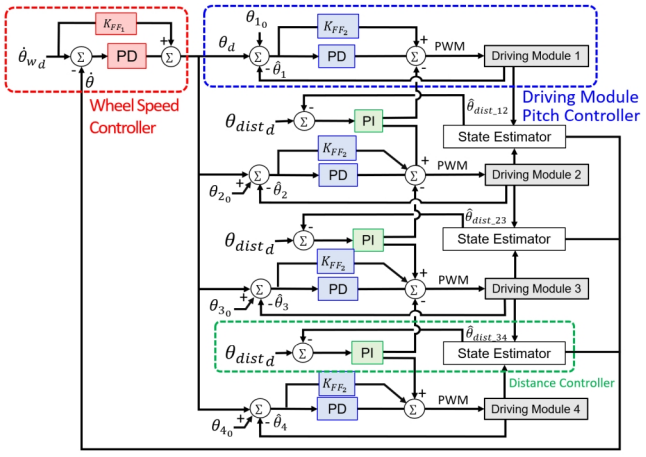

(a) Driving speed controller

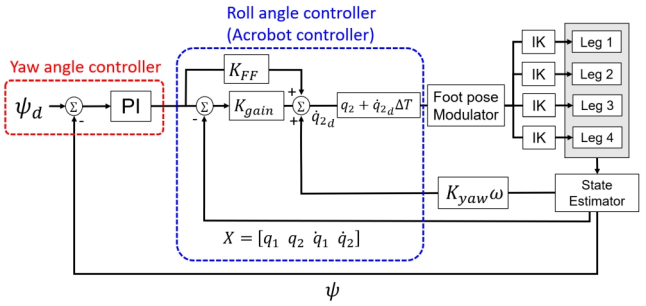

(b) Balancing/steering controller

Fig. 5: Decoupled Control Architecture

are treated as static values in the legs' inverse kinematics calculations, instead of being dynamically controlled for leg movement.

Since the legs must lift the robot's body during quadrupedal walking, it is important to make the system lightweight and compact. Therefore, the main battery (Li-Po 4s 750mAh) is strategically placed inside the second linkage of the leg, serving as part of the frame and effectively using the battery space as depicted in Fig. 2a. Additionally, an auxiliary battery (Li-Po 4s 350mAh) is placed on the body of each driving module. Consequently, the robot system has a total battery capacity of 4400mAh, ensuring extended operational time. In addition, the eight parallel-connected batteries enable hot-swapping without shutting down the robot system.

Having four articulated legs with linkages and actuators poses a challenge for quadrupedal motion, as it demands higher torque from the leg motors to support the robot's weight. To address this, the lengths of the leg links were optimized for effective balancing in driving mode and efficient use of motor power during walking. The details of this optimization process are detailed in the following section.

III. Controller

A. Driving Controller

Fig. 5 presents the control architecture consisting of two decoupled controllers for the driving mode of the Ringbot Quad, which are improved from the controller of the two-legged version. Where $\dot{\theta}_{w_d}$ is the desired wheel speed, θ_d is the desired pitch angle of the driving modules θ_{i_O} is a constant pitch angle offset for each driving module, $\hat{\theta}_{dist_{ij}}$ is the estimated distance between driving module i and adjacent module j.

The driving speed controller is responsible for the movement of the driving modules within the ring, to track the desired speed command. It is based on the basic principle of the monocycle mechanism, which dictates that the wheel continually rolls in the direction that positions the CoM at the lowest equilibrium. The inherent pitch stability provided by the metacentric weight distribution (where the CoM is below the object's rotational axis) intuitively guides the inclination of the driving modules' pitch angles to generate the necessary torque for wheel propulsion.

However, synchronizing the four driving modules is also critical for stable driving performance. The differing configurations, masses, and friction with the rails necessitate robust control for the synchronized motion of all driving modules. Without it, discrepancies could result in unwanted vibrations, thereby undermining the system's stability. To address this, the speed controller is divided into three main components: an outer loop wheel speed feedback controller, individual pitch controllers for each driving module in the inner loop, and a distance controller that ensures constant spacing between adjacent driving modules.

Rather than directly controlling the speed of the driving module motors through wheel speed feedback, the current controller maintains a smooth driving performance by ensuring consistent distances between the driving modules. Additionally, the speed controller can position the driving modules within the wheel by setting a desired speed of zero and modifying the space between adjacent modules.

While the speed controller in Fig. 5a controls the movement of the driving modules, the controller in Fig. 5b controls the lateral shift movements of the legs during the driving mode for balancing and steering. The controller is inspired by the control of the underactuated system, Acrobot [13]. Acrobot is an underactuated 2-DOF inverted pendulum with the actuator on the second link, a deviation from typical models with actuators on the first joint. As shown in Fig. 3b, the lateral dynamics of Ringbot Quad can be approximated to the Acrobot model by considering the wheel's ground contact point as a passive 1-DOF revolute joint (the first joint of the Acrobot model without torque), and the four legs as the second linkage with a lumped mass connected to the first linkage via an active 1-DOF revolute joint.

For balancing control, only the second joint of each leg is actively controlled, while the first joint is held at a fixed angle of zero. This configuration allows each leg to function as an actively controlled inverted pendulum, shifting CoM in only sideways. To model the four legs as a single lumped linkage, the angle between adjacent legs is kept constant.

Despite the complex underactuated nature of the Acrobot, many studies have proven its capability to maintain upright equilibrium with state-feedback controllers like

Linear–quadratic regulators (LQR) [14]–[17]. Similarly, the Ringbot system achieves balance under external disturbances by adjusting the legs' lateral positions based on the robot's state. As depicted in Fig. 5b, the roll angle controller functions as a state feedback controller, using the states of links 1 and 2 to calculate the desired speed of joint 2, $\dot{q}_{2_d}$, using state feedback gain. Since the leg motors operate in position control mode, the system computes the desired speed from the state feedback controller instead of calculating torque and then derives the desired position of joint 2 through numerical integration, aligning with the precise control requirements of the motors.

Subsequently, the foot pose modulator calculates each leg's foot position from the simplified model, ensuring the leg poses are mirror images around link 2. This position is mapped using parameters r, the distance from the origin of joint 2 to the foot, and α, the angular offset from link 2, as illustrated in Fig. 3b.

When the wheel is stationary, the system functions like an Acrobot, with the implemented controller maintaining balance for upright equilibrium. However, unlike a typical Acrobot system, when the wheel starts rolling, it generates a gyroscopic force that stabilizes the roll angle, meaning that joint 1 experiences a torque acting against its velocity. This gyroscopic torque allows the wheel to maintain balance at a non-zero roll angle, resulting in steering due to the precession effect. Leveraging this principle, we've devised a yaw angle feedback controller for the outer loop and a roll angle controller for the inner loop, enabling the same controller to manage both balancing and steering when the robot is in driving mode.

B. Quadruped Walking

Ringbot quad is also capable of performing quadruped walking locomotion while completely lifting its body. This not only enhances its adaptability but also significantly broadens its operational scope, especially in unstructured terrains. With this walking ability, the robot is better equipped to navigate challenging terrains where wheeled driving might struggle. Examples of such terrains include staircases, rugged landscapes, and areas littered with obstacles. Furthermore, this dual functionality of driving and walking ensures that the Ringbot remains versatile, able to switch between modes depending on the environment and the task.

For quadrupedal locomotion, the robot employs two distinct gaits: the trot gait for faster movement and the walking gait for enhanced stability.

1) Trot gait: The Trot gait is illustrated in Fig. 6a. In this gait, legs in diagonal pairs move together. A blue color in the diagram indicates the swing phase, while the support phase is depicted in white. As the legs in the swing phase move their feet to the subsequent stepping point, the legs in the support phase propel the robot's body toward the forward direction. While the trot gait might seem less stable with only two legs supporting the body at any given time, it provides quicker maneuverability compared to the more sequential quadruped walking gait. Moreover, the increased pace of the trot gait

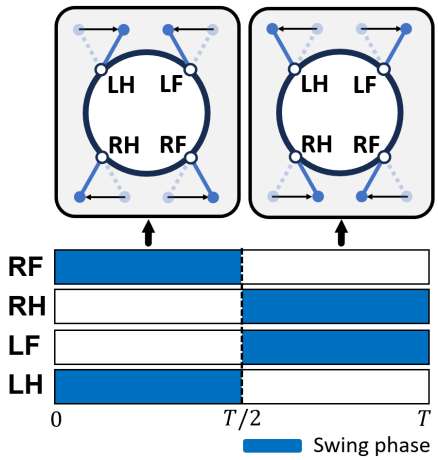

(a) Trot gait

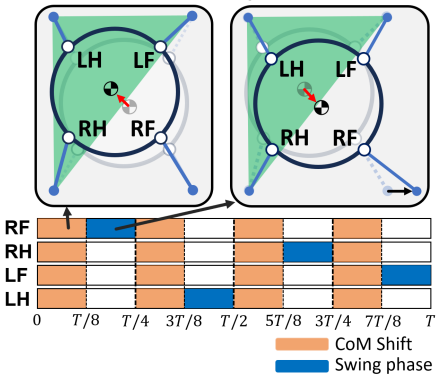

(b) Walking gait

Fig. 6: Gait patterns of Ringbot Quad

generates momentum that contributes to the robot's overall balance.

2) Walking gait: In quadrupedal locomotion, the walking gait pattern is recognized for its stability due to the consistent contact of at least three feet with the ground, forming a large support polygon. It involves one leg at a time executing a stepping action while the other three legs contribute to propulsion in the targeted direction. This stepping sequence rotates through all four legs, creating a continuous, coordinated movement pattern. A challenge arises due to the weight distribution of the legs and the unique ring-shaped structure of Ringbot Quad. The majority of the mass is located around the wheel's perimeter, while the interior remains hollow. The legs are a significant portion of the robot's overall mass, causing the wheel structure to take a considerable bending load with each step. As a result, when a leg swings forward, the projected CoM often extends beyond the support polygon created by the other three legs, making the robot lose balance. To resolve this, an additional CoM shift phase is added before each foot's swing phase, nudging the CoM closer to the centroid of the three-leg support polygon. This adjustment ensures that the robot moves securely in its quadrupedal walking motion, minimizing the risk of imbalances or tipping. Fig. 6b illustrates a single cycle of the walking gait, with the subsequent diagram detailing each phase and visualization of the CoM shift and subsequent

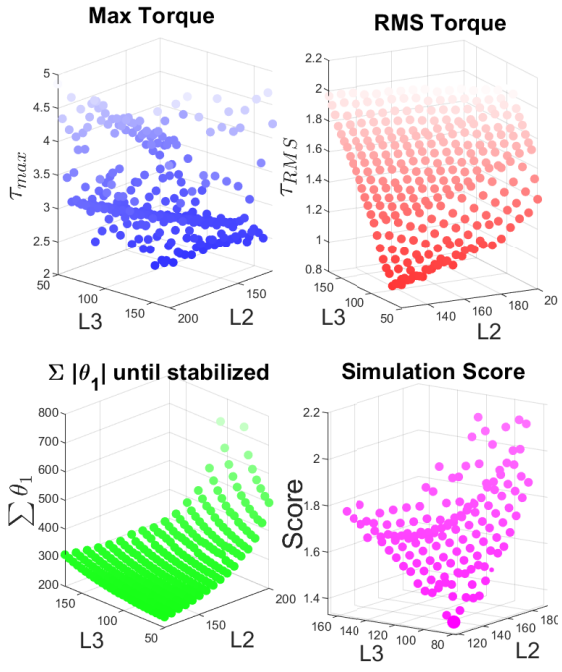

Fig. 7: Grid-Search optimization result. Best score at [$L_2 = 125$ mm, $L_3 = 100$mm]

swing phase movement of the right front foot.

IV. Leg Link Length Optimization

For the Ringbot Quad, the torque capacity on each leg motor is a critical concern because these motors must support the robot's entire weight when the robot is in walking mode. As the total weight of the robot is 3.9 kg, which causes significant load to the leg servo motors, therefore improper leg design causes overload at the motors, preventing the robot from walking. To address this, an exhaustive grid-search method was used to determine optimal leg link lengths by testing various combinations of the leg linkages in certain ranges.

The walking simulations were carried out using MATLAB2022a Simscape Multibody, where the robot executed the walking gait with fixed gait parameters such as stride, step time, and step height. Each simulation varied leg linkage lengths and set initial foot positions to maintain consistent motor angles in different cases. This method identified the leg length combination that uses the least amount of torque during the walking motion.

As changes in leg linkage lengths impact the legs' mass and inertia, and consequently the balancing performance, the optimization also takes account for balancing, trying to find the link length combination that ensures the least motor torque consumption while walking as well as good balancing performance. The balancing simulation was implemented by making a dynamics simulation model in a MATLAB script for the simplified Acrobot model introduced in Section III. The mass and inertia of Link 2, representing a simplified model of the legs, were defined based on each link length set being evaluated. Each simulation began with non-zero initial

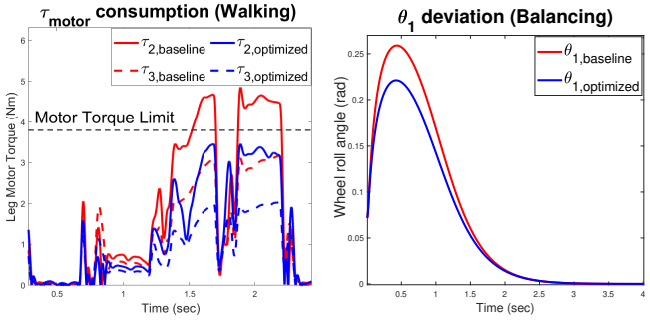

(a) Motor torque of a leg during a quadruped walking cycle

(b) Wheel roll angle on the balancing simulation with $\theta_{1_0} = 4°$.

Fig. 8: Comparison between the baseline link lengths [$L_2 = 135.25$mm, $L_3 = 140.25$mm] and the optimized link lengths [$L_2 = 125$ mm, $L_3 = 100$mm]

conditions for position and velocity at joint 1, indicative of the wheel state, to monitor the rate at which these values could stabilize to zero, implying the robot had achieved balance.

The simulation served as a design-optimization tool rather than a high-fidelity locomotion simulation. To facilitate the exhaustive grid-search, we utilized simplified model that omitted the structural compliance of the hardware. While this approach required empirical tuning to bridge the resulting sim-to-real gap in the controller, it provided a clear, evidence-based rationale for selecting the optimal leg link lengths (L_2, L_3).

$$
\begin{aligned}
&\underset{L_2,\ L_3}{\textit{minimize}} \quad \frac{\Sigma_{i=1}^{4}\mathrm{RMS}(\tau_{i,j})}{\max(\tau_{RMS})} + \frac{\Sigma\theta_1}{\max(\Sigma\theta_1)} \\
&\text{subject to} \\
&L_2 = \{x \,|\, 125 \le x \le 200\ mm, x = 125 + 5n\}, \\
&L_3 = \{x \,|\, 60 \le x \le 180\ mm, x = 60 + 5n\}, \\
&L_2 + L_3 - L_1 < R_i, \\
&\tau_{i,j} < \tau_{stall}, \\
&\{\theta_{\text{leg}} \in \mathbb{R} \,|\, 0 \le l_{\text{stride}} \le 60\ mm, 0 \le h_{\text{foot}} \le 80\ mm\}
\end{aligned}
\tag{1}
$$

In Eq. 1, the initial term represents the normalized total of the Root Mean Square (RMS) motor torque for all leg motors. This metric is used for identifying leg linkage lengths that utilize the least torque during quadruped walking. The following term in the equation originates from the Acrobot balancing simulation, which measures the cumulative ring roll angle over the total simulation duration. This measurement indicates the speed at which the model achieves stabilization from a non-zero equilibrium.

The optimal leg linkages were identified through a grid search optimization within the boundaries and the interval defined by the conditions. The candidate lengths' upper and lower limits were set based on component sizes and the wheel's dimensions. Several constraints were imposed during optimization to ensure realistic simulations and to eliminate infeasible iterations. Any linkage combination exceeding the joint's stall torque was disregarded. Leg lengths were also

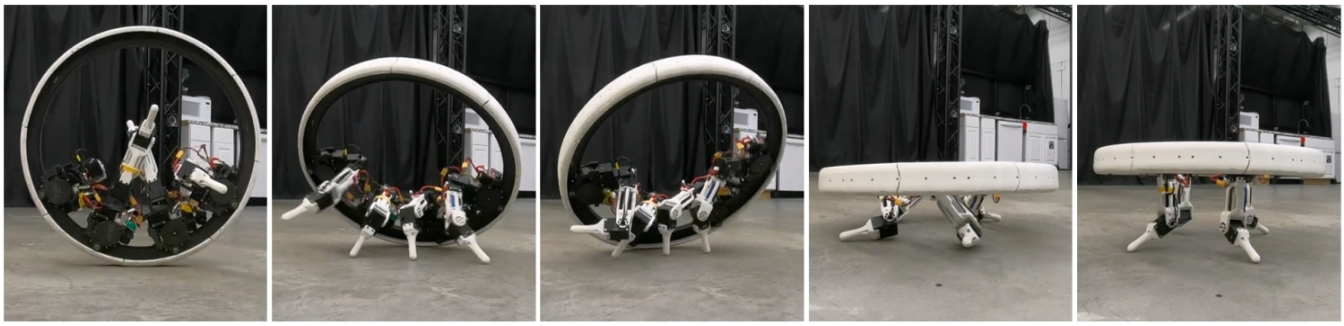

Fig. 9: Snapshots of Ringbot Quad transitioning from driving mode to quadruped walking mode

confined to ensure fully extended legs remained within the wheel's inner rim. Furthermore, cases without an inverse kinematics solution for a given footstep stride and height range were excluded.

In Fig.7, the optimization result is presented. The data collected from both the walking and balancing simulations consistently indicate a preference for shorter link lengths in terms of L_2 and L_3. The optimal link length combination was identified as $L_2 = 125$mm and $L_3 = 100$mm, recorded the lowest score in the grid. A comparative analysis between the baseline link lengths, as employed in the two-legged Ringbot, and the newly optimized link lengths can be observed in Fig.8. The results underscore a marked enhancement in both the efficiency of torque consumption and the duration required for balancing. In particular, Fig. 8a illustrates that the leg motor torque surpasses the motor's stall torque as specified by the manufacturer when using the original link lengths. However, with the optimized link lengths, this issue is mitigated, resulting in an overall reduction in torque consumption.

V. Results

A. Driving

The Ringbot Quad's driving performance was tested on the actual hardware, operating tetherless with a remote joystick control via a WiFi network. The yaw angle command was fixed at zero, while the speed command incrementally reached the robot's maximum of 4km/h, held for 6 seconds, then decelerated. Experiment results in Fig 10 show the robot successfully tracking the speed command and achieving a peak speed of 4.29km/h. The absolute orientation of the wheel measured by IMUs only showed a small fluctuation in the robot's roll angle, less than 4 degrees. However, as the robot decelerated, a slight drift in the heading direction was noted, indicating less stable driving performance at lower speeds where gyroscopic forces are insufficient for stabilization.

B. Quadruped walking

The Ringbot Quad can transition from driving to quadruped walking mode without human intervention. This autonomous capability enables the robot to recover from a loss of balance or navigate terrains insurmountable for

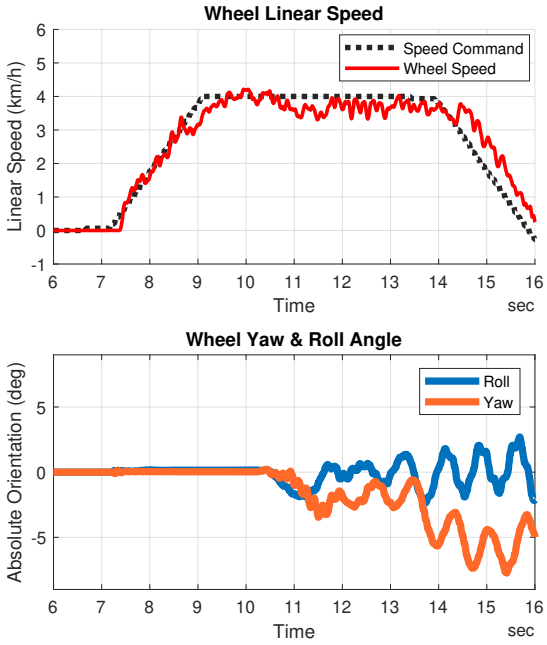

Fig. 10: Hardware experiment result of straight driving

monocycle driving by switching to a stable quadrupedal configuration. As shown in Fig. 9, the robot maneuvers its legs to one side to induce a controlled fall. The legs then contact the ground, positioning the wheel parallel to the surface and extending for quadrupedal locomotion. This adaptability ensures the robot remains functional in dynamic environments where driving alone is insufficient.

Both trot and walking gait patterns were tested on the actual robot hardware. At maximum leg motor speed, the robot performed a trot gait with a step period of 1 second, stride of 60 mm, and trotting speed of 120 mm/s. In walking gait, it reached a step period of 4 seconds, a stride of 60 mm, and a walking speed of 30 mm/s, marking the optimal performance for each gait. Demonstrations of these walking motions are included in the supplementary video.

A simulation study was conducted to demonstrate the adaptability and versatility of the Ringbot Quad, particularly when it comes to navigating challenging terrains like stairs. Stairs often pose significant difficulties for wheeled mechanisms due to their abrupt elevation changes. To mimic real-

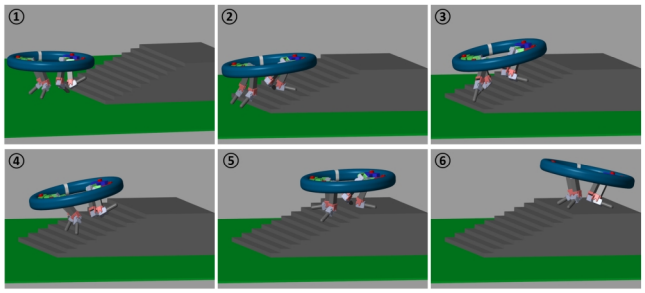

(a) Snapshots of the stair climbing simulation

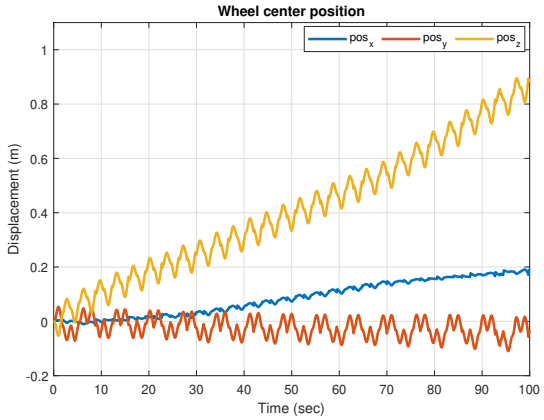

(b) The robot position displacement while climbing up the stairs

Fig. 11: Stair Climbing Simulation Result

world challenges, the simulation, developed in MATLAB 2022a Simscape Multibody, presented stairs with a profile of a 20 mm rise (height) and a 55 mm run (length) for each step. Fig. 11 showcases the results of this simulation, offering snapshots of key moments during the robot's ascent and tracking the position displacement of the robot's origin about the ground level. The simulation model of Ringbot Quad successfully ascended 10 stairs, highlighting its potential to overcome such obstacles even with the legs with limited DoF.

VI. Conclusion

This paper presents Ringbot Quad as a novel proof-of-concept for a hybrid mobile robot that fuses monocycle driving with legged locomotion within a unified system. The core contribution lies in a unique architecture that incorporates four independent, 3-DOF legged modules inside a single monocycle wheel , enabling versatile movements such as dynamic stabilization, active steering, and transformable quadrupedal walking. By characterizing the performance in each mode , this study demonstrates how the monocycle form factor can achieve superior adaptability in diverse environments.

The current prototype primarily focuses on validating the fundamental feasibility of the proposed concept by employing a compact-scale hardware architecture with servo motors. While this setup successfully demonstrates the system's core locomotion paradigm, it also encounters specific performance boundaries inherent to the chosen hardware scale. These include limitations in both the maximum driving speed and the walking speed due to the power constraints of the small-scale actuators. Nevertheless, these experimental results establish a critical performance baseline for this unique form factor, providing a solid foundation for future high-performance iterations with scaled-up hardware.

Looking ahead, this work sets the stage for a new class of scalable mobile robots. Future iterations will focus on larger-scale designs to accommodate higher-performance motors, which will significantly enhance driving stability, balancing, and walking capabilities beyond the current prototype's limits. Furthermore, these advanced platforms will integrate comprehensive perception systems to transition from remote-controlled locomotion to fully autonomous navigation in complex, dynamic urban settings.

References

[1] A. Stentz, H. Herman, A. Kelly, E. Meyhofer, G. C. Haynes, D. Stager, B. Zajac, J. A. Bagnell, J. Brindza, C. Dellin *et al.*, "Chimp, the cmu highly intelligent mobile platform," *Journal of Field Robotics*, vol. 32, no. 2, pp. 209–228, 2015.

[2] H. Bae, I. Lee, T. Jung, and J.-H. Oh, "Walking-wheeling dual mode strategy for humanoid robot, drc-hubo+," in *2016 IEEE/RSJ International Conference on Intelligent Robots and Systems (IROS)*, 2016, pp. 1342–1348.

[3] S. Karumanchi, K. Edelberg, I. Baldwin, J. Nash, J. Reid, C. Bergh, J. Leichty, K. Carpenter, M. Shekels, M. Gildner *et al.*, "Team robosimian: semi-autonomous mobile manipulation at the 2015 darpa robotics challenge finals," *Journal of Field Robotics*, vol. 34, no. 2, pp. 305–332, 2017.

[4] M. Bjelonic, P. K. Sankar, C. D. Bellicoso, H. Vallery, and M. Hutter, "Rolling in the deep – hybrid locomotion for wheeled-legged robots using online trajectory optimization," *IEEE Robotics and Automation Letters*, vol. 5, no. 2, pp. 3626–3633, 2020.

[5] H.-Y. Wang, L.-J. Chen, W.-S. Yu, and P.-C. Lin, "A wheel to leg transformation strategy in a leg-wheel transformable robot," in *2023 IEEE/ASME International Conference on Advanced Intelligent Mechatronics (AIM)*, 2023, pp. 293–298.

[6] Z. Huang, W. Jia, Y. Sun, S. Ma, Z. Wang, H. Pu, and Y. Tian, "Design and analysis of a transformable spherical robot for multi-mode locomotion," in *2017 IEEE International Conference on Mechatronics and Automation (ICMA)*, 2017, pp. 1469–1473.

[7] C. W. Bert, "Dynamics and stability of unicycles and monocycles," *Dynamics and Stability of Systems*, vol. 5, no. 1, pp. 30–35, 1990.

[8] S.-J. Tsai, E. Ferreira, and C. Paredis, "Control of the gyrover. a single-wheel gyroscopically stabilized robot," in *Proceedings 1999 IEEE/RSJ International Conference on Intelligent Robots and Systems (IROS)*, vol. 1, 1999, pp. 179–184 vol.1.

[9] Y. Ou and Y. Xu, "Stabilization and line tracking of the gyroscopically stabilized robot," in *Proceedings 2002 IEEE International Conference on Robotics and Automation (ICRA)*, vol. 2, 2002, pp. 1753–1758 vol.2.

[10] P. Cieslak, T. Buratowski, T. Uhl, and M. Giergiel, "The mono-wheel robot with dynamic stabilisation," *Robotics and Autonomous Systems*, vol. 59, no. 9, pp. 611–619, 2011.

[11] M. Forouhar, M. H. Abedin-Nasab, and G. Liu, "Introducing gyrosym: A single-wheel robot," *International Journal of Dynamics and Control*, vol. 8, pp. 404–417, 2020.

[12] K. G. Gim and J. Kim, "Ringbot: Monocycle robot with legs," *IEEE Transactions on Robotics*, vol. 40, pp. 1890–1905, 2024.

[13] M. Spong, "The swing up control problem for the acrobot," *IEEE Control Systems Magazine*, vol. 15, no. 1, pp. 49–55, 1995.

[14] T. Kobayashi, T. Komine, S. Suzuki, M. Iwase, and K. Furuta, "Swing-up and balancing control of acrobot," in *Proceedings of the 41st SICE Annual Conference. SICE 2002.*, vol. 5, 2002, pp. 3072–3075 vol.5.

[15] Y. Daud, A. Al Mamun, and J.-X. Xu, "Dynamic modeling and characteristics analysis of lateral-pendulum unicycle robot," *Robotica*, vol. 35, no. 3, pp. 537–568, 2017.

[16] S. Bortoff and M. Spong, "Pseudolinearization of the acrobot using spline functions," in *[1992] Proceedings of the 31st IEEE Conference on Decision and Control*, 1992, pp. 593–598 vol.1.

[17] J. Hauser and R. M. Murray, "Nonlinear controllers for non-integrable systems: the acrobot example," 1990.